A Study on the Relationship between Spore Count and Color Difference Values during the Mildewing Process of Paper Wine Boxes

Ke Li,[a] Junying Ji,[a] Yuheng Jiang,[a] Ruo Liu,[a] Qin Yang,[a] Ruijie Huo,[b] Qianqian Yao,[b] Yubo Dou,[b] and Haiyan Song ,[b,c]*

Changes in the number of mold spores and the color difference values of cardboard were evaluated during the molding process of paper wine boxes. The experiment utilized three types of cardboard: single white industrial paperboard (Q), grey-offset paperboard (S), and grey-coated white paperboard (T), along with nine strains of mold collected from mold-contaminated paper wine box samples. The molds were identified using both morphological and molecular techniques. These nine strains were inoculated on the surface of the cardboard and incubated at 28 °C and 98% relative humidity for 28 days to assess the number of mold spores and the color difference values. The results indicated a gradual increase in both the number of mold spores and the color difference values over the 28-day period. The total spore count was highest on cardboard type Q, followed by S and T (T < S < Q), whereas the average color difference value followed the reverse order (S < Q < T). A linear correlation model between the color difference value and spore count was developed using Matlab software to fit the data, providing a method to predict the number of mold spores based on the color difference values of the cardboard.

DOI: 10.15376/biores.20.2.3315-3328

Keywords: Paperboard; Spore count; Color difference; Predictive modeling; Microbial identification

*Contact information: a: Luzhou Laojiao Co., LTD, Sichuan, China; b: Tianjin University of Science and Technology, Tianjin, China; c: State Key Laboratory of Bio-based Fiber Materials, Tianjin University of Science & Technology, Tianjin 300457, P.R. China; *Corresponding author: songhaiyan00@126.com*

INTRODUCTION

The concept of green development has led to a growing focus on sustainability (Su and Zhao 2023). Paper-based packaging is widely favored due to its recyclability and environmental sustainability. However, under hot and humid conditions, paper packaging is prone to fungal contamination.

Fungi are cellulase-producing microorganisms capable of degrading paper by secreting a range of enzymes, which allows them to thrive on paper substrates. This represents a significant threat to the integrity of paper packaging (Menicucci *et al.* 2023). Molds, in particular, produce mycotoxins, which are secondary metabolites generated by certain fungal species. To date, over 400 distinct mycotoxins have been identified, and their concentrations often exceed safe limits, posing substantial risks to both human health and the environment (Sun *et al.* 2023).

Several studies have previously examined the mildew issue in paper packaging materials. For instance, Zaffora *et al.* (2024) developed a new model to estimate the time required for mold growth on novel paper-based materials, aiming to establish an alternative statistical framework for assessing the impact of relative humidity and temperature on mold proliferation. Kosel *et al.* (2024) demonstrated that reflectance-mode FTIR spectroscopy could be an effective tool for the rapid detection and monitoring of mold biofilms on paper materials. Gobakken and Westin (2008) investigated the inhibition of mold growth on paper surfaces through three different coating systems. Gradeci *et al.* (2017) conducted a comprehensive literature review on the development of criteria and models for characterizing mold growth in paper packaging materials. They discussed the findings of experimental studies on factors influencing mildew growth. However, these studies primarily focused on the effects of conventional single factors, such as temperature, humidity, and anti-mold coatings, on cardboard mold, with relatively limited in-depth exploration of the relationship between mold spore count and the color difference of cardboard.

There is a growing research trend to develop mathematical prediction models that integrate digital technologies and experimental methodologies (Kaminski *et al.* 2017; Banwarth-Kuhn and Sindi 2020; Quan *et al.* 2021). For instance, Jia *et al.* (2024) explored the relationship between radial color differences and the metabolites of wood materials, revealing a consistent radial pattern in both color difference and metabolic profile. Similarly, An *et al.* (2023) employed near-infrared spectroscopy to create a prediction model for walnut mold, enabling non-destructive detection of mold growth. Liu *et al.* (2024) proposed an improved algorithm for detecting corn kernel breakage and mold, based on an enhanced YOLOv5s model, which increased the average precision (AP) for the identification of these issues. However, there remains a relative lack of systematic studies on the relationship between cardboard color difference and mold growth in the existing literature. Given this gap, it is important to investigate the correlation between the number of mold spores and the color difference values of cardboard during the mildew development process in paper wine boxes. The variation in cardboard color difference could serve as an indicator of mold progression. A thorough understanding of this relationship is expected to facilitate the development of prediction methods that can inform mold prevention strategies, thus contributing to the stable growth of the liquor packaging industry.

This study investigated the presence of moldy wine boxes stored in wineries within specific regions. There are usually three kinds of cardboard for wine boxes, they are single white industrial paperboard, grey-offset paperboard and grey-coated white paperboard. A single white industrial paperboard refers to a composite material comprised of grey board and grey-coated white paperboard. Grey-offset paperboard refers to a composite material consisting of gray board with double-sided offset paper. Grey coated whiteboard paper had a kind of white and smooth front, whereas the back was mostly grey board. Nine strains of mold isolated from the cardboard of these wine boxes were identified and characterized. The study then quantified the number of mold spores and assessed the color difference values of three types of cardboard specimens. Finally, a mathematical model was developed to analyze the impact of mold growth on the color difference value of the cardboard. This model systematically elucidates the underlying mechanism governing the relationship between mold growth and color variation, offering novel insights and approaches for mold prevention in the context of liquor packaging.

EXPERIMENTAL

Materials

Strains were obtained from the moldy paper wine boxes in the warehouse of a winery. Single white industrial paperboard, grey-offset paperboard, and grey-coated white paperboard were obtained from the paper wine boxes in the warehouse of a winery.

Tapioca starch was provided by the cardboard manufacturer; EDTA was purchased from a paperboard manufacturer. *Aspergillus niger*, *Penicillium oxalicum*, *Penicillium extensum*, *Penicillium creeper*, and *Rhizoctonia cordata* were purchased from the Beijing Biological Institute. Fine Wart-like Fungus, *Streptochromosporidium*, Very Fine Dendrocystis, and *Dendrocystis acuminata* were purchased from the Shanghai Conservation Center for Microorganisms.

Methods for Identification and Characterization of Molds

The isolation and purification process of molds involved collecting samples from the surface of mold-contaminated paper wine boxes and storing them within a temperature range of 2 to 4 °C. The samples were then sealed and incubated at 28 °C for 2 to 5 days. Following this incubation period, individual colonies were selected and screened for molds based on their morphological characteristics and compared to control samples to identify the target molds (Matysik *et al.* 2008). Colony growth was monitored daily, and colonies exhibiting distinct morphological features were selected for further purification. The inoculation process was repeated until a single mold strain was isolated (Yu *et al.* 2019).

The identification of mycobacteria commenced with the observation of their morphological characteristics, which was conducted using a 400x light microscope (model JSM-IT300LV, JEOL, Kyoto, Japan) (Saif *et al.* 2020). For the biological identification of mold molecules, genomic DNA was extracted using a modified pitcher method (Cheng *et al.* 2023). Polymerase chain reaction (PCR) (model 960, Hangzhou Jingge Scientific Instrument Co., Ltd.) was employed to amplify the 18S rDNA of the mycobacteria. Molecular identification was performed using the universal primers ITS1 and ITS4. The PCR products were subsequently sequenced and subjected to bioinformatic analysis. The 18S rDNA sequences were compared and phylogenetically analyzed utilizing Kimura's 2-parameter model and Bootstrap resampling techniques (Blount *et al.* 2016; Lõoke *et al.* 2017; Zasada 2020).

Preparation of Moldy Cardboard Samples

First, the mold lyophilized powder was activated and inoculated in Potato Dextrose Agar (PDA) medium for five to seven days. Subsequently, a mold suspension with a concentration of 2×10^6 (CFU/mL) was prepared and stored in a refrigerator at -4 °C. The mold suspension was uniformly sprayed on the surface of the cardboard, and the treated and control samples were subsequently placed in an incubator at a temperature of 28 °C and a relative humidity of 95% for mold incubation.

Test Method for the Number of Mold Spores

Mold spores were scraped from an area of 1 cm^2 on the surface of the cardboard samples on days 1, 7, 14, 21, and 28. A suspension was prepared, and the spores were transferred to a test tube containing 10 mL of sterile water and diluted in a 10^{-1} to 10^{-4} gradient. The diluted suspension was added dropwise to a hemocyte counting plate and left to stand for 5 to 10 min for the counting of mold spores. Five parallel experiments were

performed for each sample. The mold spores were counted using Eq. 1 (Higashijima *et al.* 2012),

$$M=\frac{A}{80}\times 400\times 1000\times B \quad (1)$$

where M denotes the number of mold spores per unit volume (units/mL), while A represents the total number of spores counted in 80 counting cubes (units/μL). The value 400 indicates the number of counting cubes used in units, and B represents the dilution ratio of the mold spore suspension. The color measurement adopted the CIE L*a*b* color system. In the color measurement, a standard observer angle of 10 degrees was used. A D65 standard light source was assumed.

Test Method for Color Difference Value of Cardboard Surface

The color difference is typically assessed using the ΔE value, which provides an effective means of evaluating the impact of the mold growth process on the color of cardboard. This is achieved by comparing the color difference between the sample and the reference standard, thereby facilitating relevant calculations for the evaluation (Morsy and Holiel 2023). Cardboard samples, along with blank control samples, were removed from a constant temperature and humidity incubator on the 1st, 7th, 14th, 21st, and 28th days of the experiment.

The color difference values were then measured using a portable colorimeter. The color difference value was calculated as follows: the blank control sample served as the reference standard, while the moldy cardboard sample was treated as the test sample. The color difference value was then computed according to Eq. 2,

$$\triangle E=\sqrt{(L_1^*-L_0^*)^2+(a_1^*-a_0^*)^2+(b_1^*-b_0^*)^2} \quad (2)$$

where ΔE represents the color difference value of the sample, L_1 is the luminance value of the test sample, L_0 is the luminance value of the standard sample, a_1 is the redness and greenness value of the test sample, a_0 is the redness and greenness value of the standard sample, b_1 is the yellowish blueness value of the test sample, and b_0 is the yellowish blueness value of the standard sample.

Establishment of Prediction Model of Mold Spore Growth Number

Relevant data were collected by monitoring the dynamic changes in spore growth and the variations in cardboard color. The data were preprocessed using the first-order difference method, as follows,

$$\Delta y_m=\frac{y(m)-y(n)}{m-n};(m,n=1,7,14,21,28) \quad (3)$$

where y represents the number of mold spores or the color difference value.

By examining the fluctuations in mold spore count on the cardboard and the corresponding changes in color difference, the first-order difference method effectively eliminated non-stationary factors, reduced data autocorrelation, and provided a more stable dataset for subsequent analysis, modeling, and prediction (Farshid Mirzaee *et al.* 2021). Building on this, statistical analysis was performed on the "spore count" and "color difference value" to investigate the relationship and patterns between these two variables. A comprehensive analysis was then conducted to evaluate and validate the model. Consequently, a predictive model for mold spore count was developed (Feng *et al.* 2015; Gao and Yang 2022; Korzilius and Schoenmakers 2023).

RESULTS AND DISCUSSION

Isolation and Identification of Molds in Paper Wine Boxes

Following the isolation and purification procedures, nine mold strains (S1–S9), each exhibiting distinct colony characteristics, were successfully obtained. Phylogenetic analysis was then conducted by constructing and sequencing the phylogenetic trees for these nine strains. The resulting sequences were further analyzed through phylogenetic tree construction, as described by Seto *et al.* (2023). The evolutionary relationships among the strains were inferred using the Neighbor-Joining method implemented in MEGA7 software (Long *et al.* 2021). Based on a comprehensive analysis incorporating both morphological observations and ITS sequence data, the following identifications were made: S1, *Aspergillus niger*; S2, *Penicillium oxalicum*; S3, *Penicillium expansum*; S4, *Talaromyces funiculosus*; S5, *Cladosporium oxysporum*; S6, *Talaromyces verruculosus*; S7, *Rhizopus stolonifer*; S8, *Alternaria alternata*; and S9, *Cladosporium tenuissimum*. The morphological characteristics of the mold strains are illustrated in Fig. 1.

Saada *et al.* (2022) succeeded in isolating and identifying 14 species of fungi from 20 Egyptian papyrus artifacts preserved at the Grand Egyptian Museum Conservation Center (GEM-CC) belonging to five different genera including *Aspergillus*, *Dendrosporium*, *Penicillium*, *Ankylostomum*, and *Ulocladium*. Similarities have existed between the results of this study and the species of strains found in the identification work conducted by us.

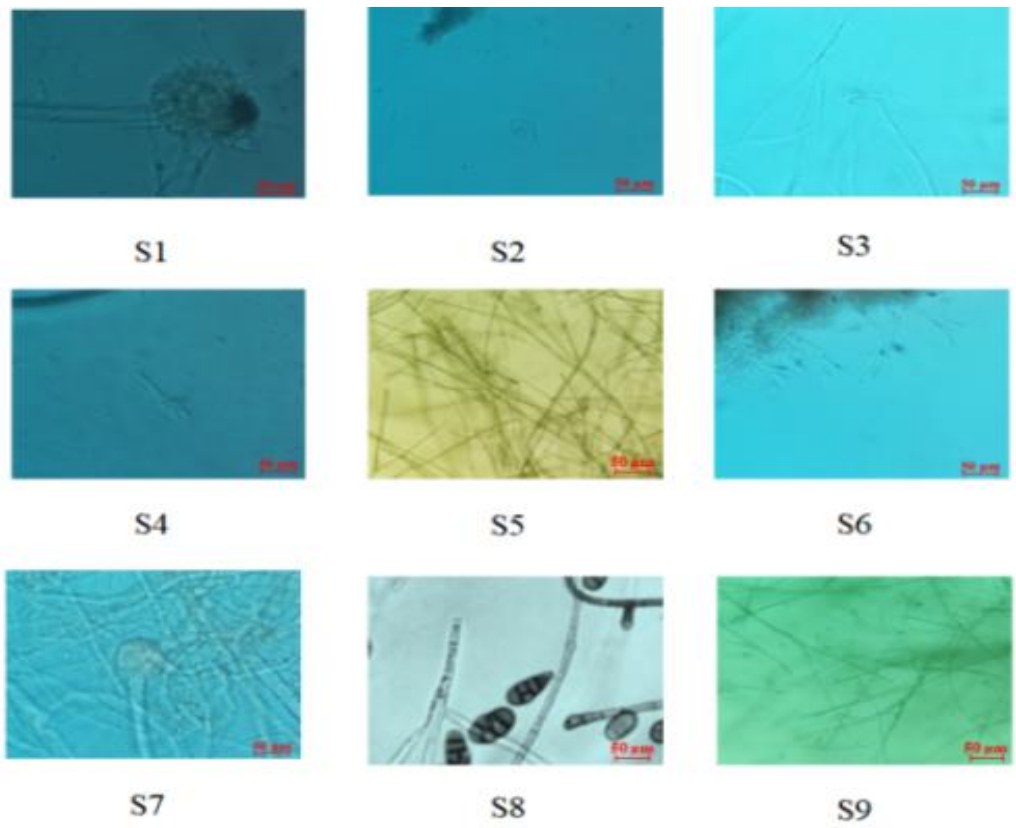

Fig. 1. Nine types of mold body morphology

The Pattern of Change in the Number of Mold Spore Growth on Cardboards

Figure 2 illustrates the growth dynamics of nine mold spores on three different cardboards during a 28-day period. In the initial stage, the growth rate of the molds was relatively slow; however, from the 14th day onwards, the growth rate of the molds accelerated significantly. Analysis of the growth data from day 14 to day 28 showed that *Penicillium expansum* had the fastest growth rate followed by *Rhizopus stolonifer* in the single white industrial paperboard. The spore count of *Aspergillus niger* reached the highest value of 2.89×10^6 CFU/mL at day 28, and the growth rate of molds showed a similar trend in grey-offset paperboard, with the spore count of *Aspergillus niger* reaching the highest value of 2.79×10^6 CFU/mL at day 28 as well. The fastest growth rate was observed in grey-coated white paperboard, with *Aspergillus niger* having the highest spore count of 1.51×10^6 CFU/mL at day 28. The maximum number of spores was 1.51×10^6 CFU/mL. The final total number of spore growth on the three different types of cardboard was in the order of grey-coated white paperboard (T) < grey-offset paperboard (S) < single white industrial paperboard (Q).

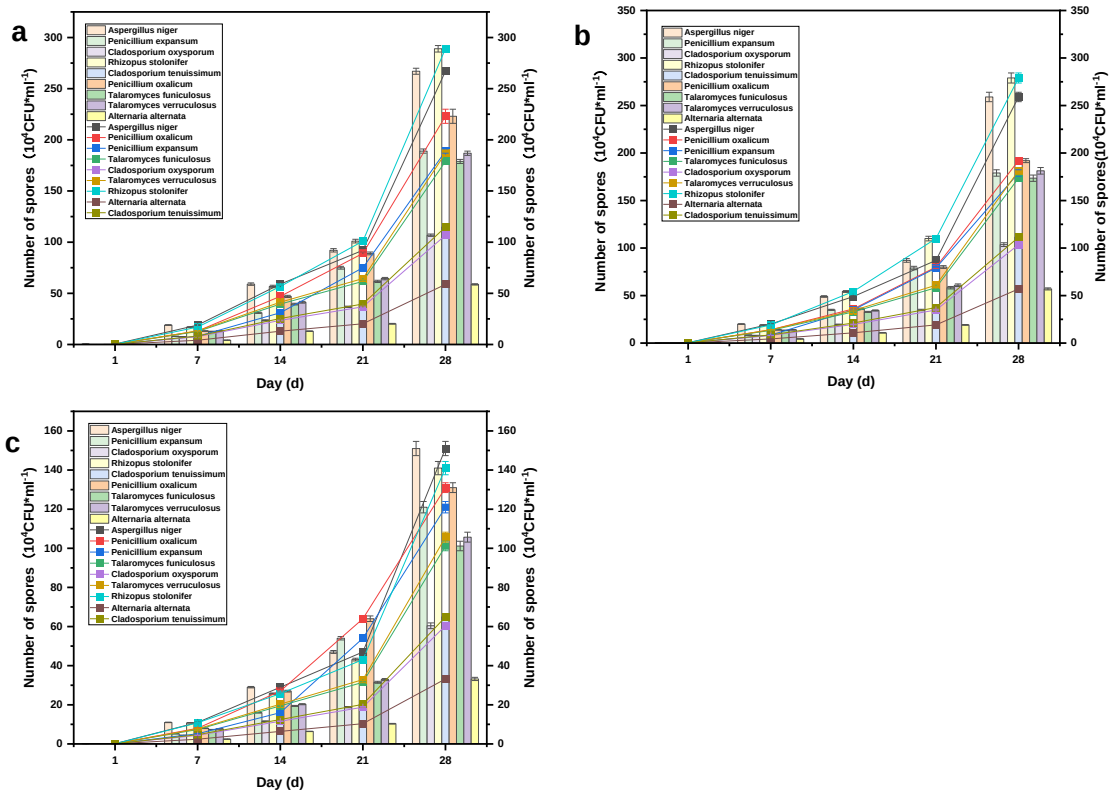

Fig. 2. Change in the number of mold spores on the surface of paperboard: single white industrial paperboard **a**, grey-offset paperboard **b**, grey-coated white paperboard **c**.

The reason for this is that mold spores begin to germinate when they come into contact with suitable environmental conditions. The organic matter on the cardboard, such as cellulose, lignin, and adhesive, provides the necessary nutrients for the mold to form the initial spores, which are in the early growth state. After the spores germinate, they form mycelium, which spreads on the surface of the cardboard, forming white mold spots. This is the mid-growth state when mycelium secretes enzymes to degrade the organic material

in the cardboard and provides more nutrition for the growth of mold. With the growth of mycelium and the accumulation of nutrients, molds begin to form sporocysts. Sporocysts will release a large number of spores after maturation. Spores spread through the air, resulting in the spread of molds and cardboard re-infection, and this time is for the growth of the middle and late state (Kwon *et al.* 2021).

Hwang *et al.* (2020) investigated a kinetic model of microbial metabolic reactions and enzymatic regulation that predicts the phenotypic behavior of microorganisms under different conditions and perturbations. The research method synthesized various factors such as growth kinetics, gene expression, and gene deletion phenotypes. The metabolite concentrations in the strains could be accurately predicted. The complexity of microbial growth and metabolic kinetics was not deeply explored in this study, which is a shortcoming of this study. Future studies should consider learning from this method (Hwang *et al.* 2020). The results of this study reveal the dynamic characteristics of mold growth on cardboard, which is crucial for developing effective mold prevention strategies and extending the service life of cardboard products. In addition, this finding provides a scientific basis for further research on mold growth dynamics and the development of novel mold prevention technology.

Effect of Mold Growth on Cardboard Color Change

Figure 3 illustrates the variation in color difference values of nine mold species on three distinct types of cardboard over a 28-day period.

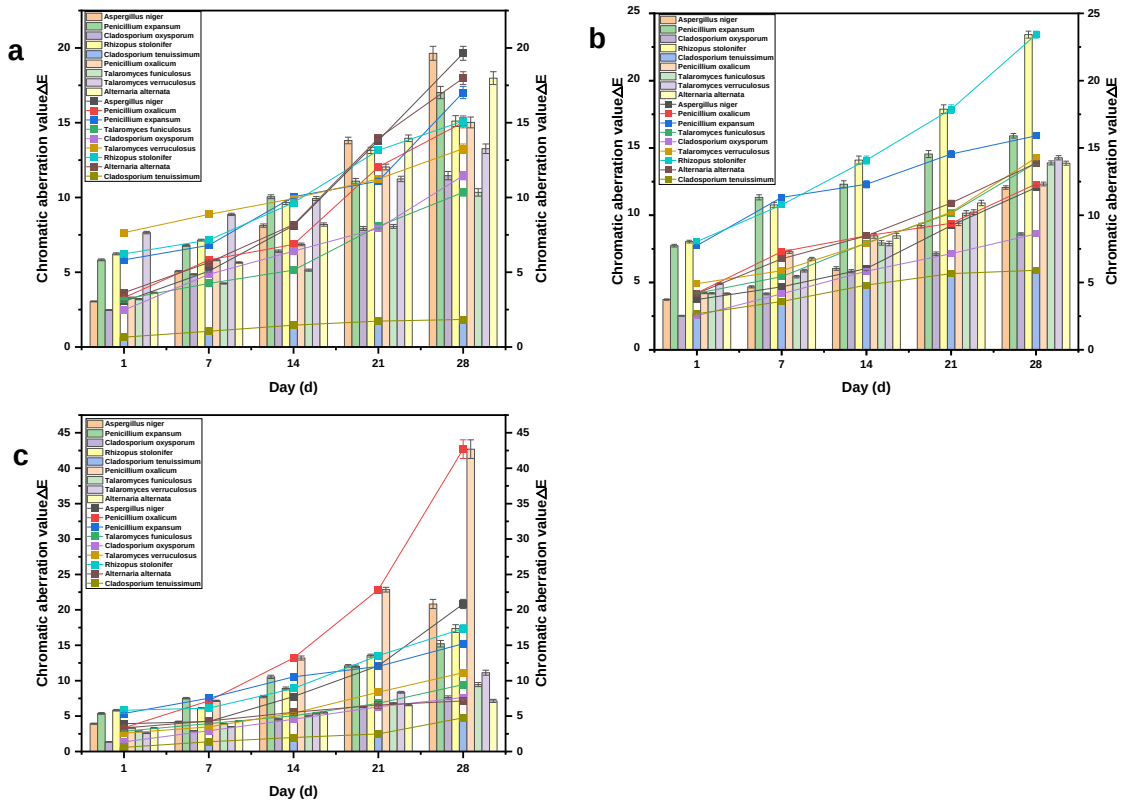

Fig. 3. The color difference values of nine types of mold growth on paperboards: single white industrial paperboard **a**，grey-offset paperboard **b**，grey-coated white paperboard **c.**

The results indicate that, over time, the color differences for all three cardboards increased as a result of mold growth. In the initial phase of the experiment, the color difference values of the cardboard generally showed a low level.

As the experiment progressed, the color difference values steadily increased, with the impact of the different mold species on the color variation showing distinct differences. On single white industrial paperboard, *Aspergillus niger* had the greatest impact. On grey-offset paperboard, very fine branching spore mold had the greatest impact. On grey-coated white paperboard, *Penicillium expansum* had the greatest impact.

According to the comprehensive analysis of Fig. 3, it is apparent that the grey-coated white paperboard color difference fluctuation was the smallest, followed by grey-offset paperboard and then single white industrial paperboard fluctuations. The average color difference value on the final paperboard was in the order of S < Q < T. The variation in color difference may be associated with the rate at which molds absorb organic matter and utilize microbial nutrient sources.

Analyzed from the Point of View of Paperboard Characteristics

The surface of grey-coated white paperboard was coated with a special coating, resulting in better smoothness and resistance to contamination. The presence of the coating reduced the probability of microbial attachment and thus helped to inhibit mold growth (Del *et al.* 2002). The grey-offset paperboard consisted of multiple layers of pulp with high pulp content and rich nutrients. It provided favorable conditions for mold growth (Revi *et al.* 2014). Single white industrial paperboard was a paperboard product white on one side and gray on the other. Although the presence of the coating inhibited mold growth, its surface coating is thin and may be slightly less resistant to mold and color stability. Therefore, the single white industrial paperboard showed a large change in color difference value during the mold growth process. The effect of mold on the color difference of industrial cardboard is closely related to raw materials, surface treatment, production process, and quality control (Sandberg 2021). However, in practice, paper/board color change is affected by a variety of factors. In addition to mold, cellulose oxidizes when exposed to light and high temperatures, causing it to change color. The characteristics of the base paper, including fiber structure, density, *etc*., as well as the composition and process of the coating material, will also affect the color of the cardboard. Therefore, these potential interference factors should be considered comprehensively when applying the forecast model to improve the accuracy of the forecast.

In a previous study, Arif Ozcan and other researchers conducted coating experiments on different paper coating formulations and measured the gloss, print gloss, ΔE color difference, contact angle, and surface energy of the paper. The study investigated the effect of dye ratios on the printing effect and gloss of aqueous inks and analyzed the types of coatings suitable for printing. The results of the study showed that the surface properties and printability of paper can be significantly improved by coating or even calendering (Ozcan *et al.* 2022). The study confirmed that paper coatings have an effect on color difference values, thus validating the analysis of the results of the present study.

Modeling of Mold Spore Growth Number and Color Difference

Figure 4 presents the fitted curves for the number of spore growth of nine mold species on Q, S, and T cardboard. The results show that the fitted curves passed through most of the data points, indicating that the model fitted the data more satisfactorily. A power function over the origin was chosen to fit the data. The model relationship equation

is Eq. 4,

$$M=aE^{b} \quad (4)$$

where M represents the number of spores, E represents the color difference value, and a and b are constant terms of the fitted curve. The results of the validation metrics in Table 1 indicate that the constructed model was able to predict the number of spores of the nine mold species on the Q, S, and T cardboards more accurately at 28 °C and 95% humidity within 28 days.

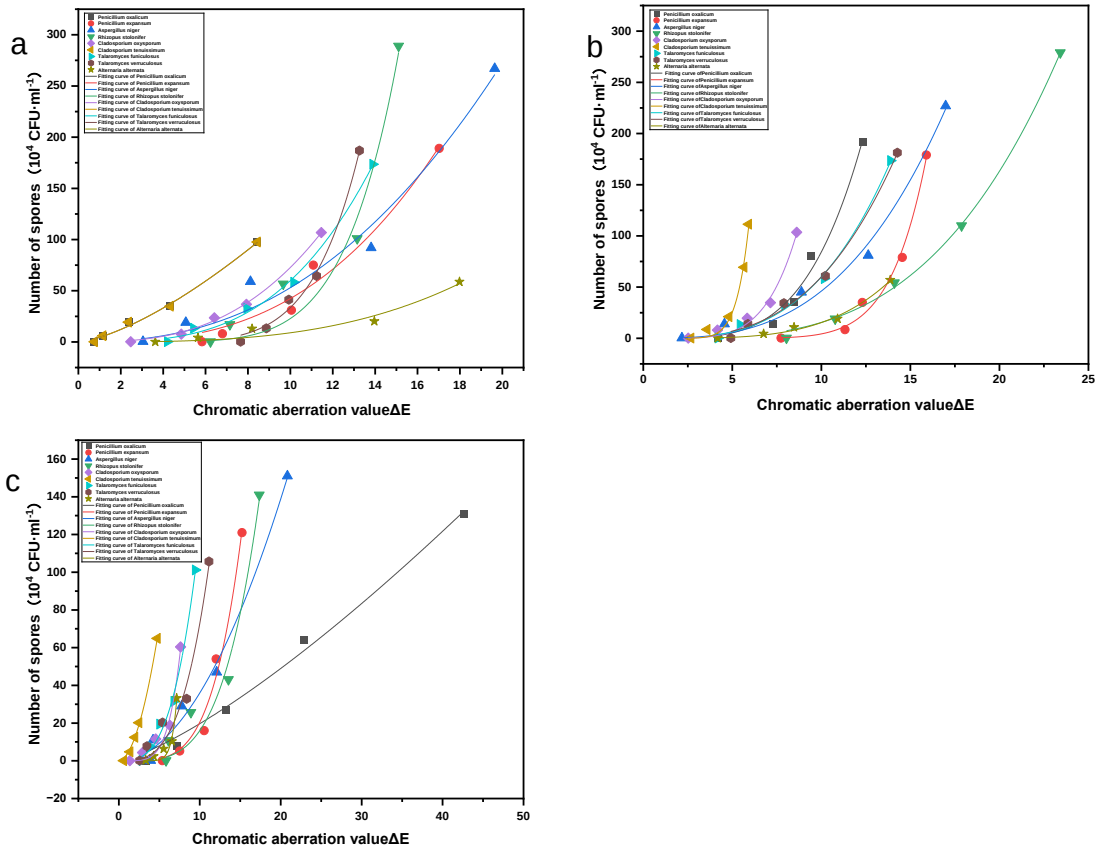

Fig. 4. Predictive models for the number of spores of nine types of fungi on (a) single white industrial paperboard, (b) grey-offset paperboard and (c) grey-coated white paperboard

The values of R^2, SSE, and RMSE (root mean square error) listed in Table 1 were analyzed. The coefficient of determination R^2 of the nine mold prediction models for the three types of cardboards ranged from 0 to 1, and the absolute coefficient values tended to be close to 1, which indicated that the models fitted the actual values well. The RMSE of the cardboards of Q ranged from 2.15 to 26.54; the RMSE of the cardboards of S ranged from 2.361 to 18.10; and the RMSE of the cardboards of T ranged from 1.33 to 11.68. The smaller the RMSE value, the higher the accuracy of the model for prediction by color difference values, and the confidence intervals (CIs) were all 95%, reflecting the high reliability of the model.

Previous studies have shown that the OpenCV vision library can be utilized for image segmentation, processing, and grayscale recognition. The growth of mold spores can be objectively assessed by the average gray value, and the mold growth model can be

constructed accordingly. There is a linear correlation between the number of colonies on the surface of the material and the grayscale value (Du *et al.* 2023).

Likewise, this study confirms that the establishment of the relationship between the number of cardboard mold spores and the cardboard color difference values is feasible.

Wang *et al.* (2024) constructed a mold growth prediction model based on temperature and relative humidity parameters. The accuracy of the model was verified. This study was limited to a specific set of temperature and humidity conditions, and future studies may consider extending the range of combinations of temperature and humidity parameters to enhance the generalizability of the model (Wang *et al.* 2024).

Table 1. Nine Types of Mold Prediction Results and Validation Indexes for Three Types of Cardboards

Board Type	Mold Name	Prediction Model	*a*	*b*	SSE	R^2	RMSE
Single white industrial paperboard (Q)	S1	$M=0.2302E^{2.362}$	0.2302	2.362	787	0.9716	20.71
	S2	$M=0.0389E^{3.182}$	0.0389	3.182	1231	0.9619	20.26
	S3	$M=0.0631E^{2.827}$	0.0631	2.827	600.9	0.9749	14.15
	S4	$M=0.0751E^{3.319}$	0.0751	3.319	764.8	0.9624	15.97
	S5	$M=0.1122E^{2.812}$	0.1122	2.812	13.94	0.9981	2.15
	S6	$M=0.0027E^{6.082}$	0.0027	6.082	147.80	0.9933	7.019
	S7	$M=0.0002E^{6.094}$	0.0002	6.094	1131	0.9610	26.54
	S8	$M=0.0062E^{3.159}$	0.0062	3.159	107.20	0.9512	5.977
	S9	$M=0.0172E^{14.431}$	0.0172	14.431	571.10	0.9319	13.80
Grey-offset paperboard (S)	S1	$M=0.0631E^{3.335}$	0.0631	3.335	483	0.9771	18.10
	S2	$M=0.0087E^{3.988}$	0.0087	3.988	367	0.9847	11.06
	S3	$M=0.0004E^{8.022}$	0.0004	8.022	230.4	0.9892	8.763
	S4	$M=0.0358E^{3.224}$	0.0358	3.224	78.2	0.9959	5.10
	S5	$M=0.0021E^{5.011}$	0.0021	5.011	82.15	0.9880	5.23
	S6	$M=0.0471E^{3.105}$	0.0471	3.105	88.45	0.9958	5.430
	S7	$M=0.0062E^{3.397}$	0.0062	3.397	73	0.9985	4.94
	S8	$M=0.0016E^{3.976}$	0.0016	3.976	16.73	0.9920	2.361
	S9	$M=0.1398E^{23.191}$	0.1398	23.191	484.90	0.9389	12.71
Grey-coated white paperboard (T)	S1	$M=0.4058E^{1.948}$	0.4058	1.948	126	0.9914	6.48
	S2	$M=0.9561E^{1.314}$	0.9561	1.314	80	0.9930	5.15
	S3	$M=0.0011E^{4.256}$	0.0011	4.256	181.2	0.9821	7.771
	S4	$M=0.0836E^{3.158}$	0.0836	3.158	53.6	0.9918	4.22
	S5	$M=0.0022E^{5.019}$	0.0022	5.019	85.04	0.9637	5.32
	S6	$M=0.0359E^{3.306}$	0.0359	3.306	206.80	0.9711	8.304
	S7	$M=0.0019E^{3.915}$	0.0019	3.915	409	0.9680	11.68
	S8	$M=0.0008E^{11.241}$	0.0008	11.241	30.73	0.9566	3.201
	S9	$M=3.4213E^{1.889}$	3.4213	1.889	5.32	0.9980	1.33

CONCLUSIONS

1. From examination of the paper wine boxes with mildew in specific areas, 9 mildew strains were identified by isolation, purification, morphology and molecular biology, which were listed as S1 to S9.
2. The number of mold spores and the cardboard color difference both increased progressively with mold growth. The growth rate of mold spores exhibited a significant increase after approximately 14 days, with the total spore count following the sequence T < S < Q. The average color difference of the cardboard was ranked in the order of S < Q < T, with grey-coated white paperboard displaying the smallest fluctuation in color difference, followed by grey-offset paperboard, and single white industrial paperboard showing the greatest variation.
3. A method for predicting the number of mold spores on single white industrial paperboard (Q), grey-offset paperboard (S) and grey-coated white paperboard (T), based on color difference was proposed. A model correlating mold spore growth with color difference was developed, enabling the prediction of mold growth on cardboard through color variation.

REFERENCES CITED

An, M., Cao, C., Wang, S., Zhang, X., and Ding, W. (2023). "Non-destructive identification of moldy walnut based on NIR," *Journal of Food Composition and Analysis* 121, 105407-105407. DOI: 10.1016/j.jfca.2023.105407

Banwarth-Kuhn, M., and Sindi, S. (2020). "How and why to build a mathematical model: A case study using prion aggregation," *Journal of Biological Chemistry* 295(15), 5022-5035. DOI: 10.1074/jbc.rev119.009851

Blount, B. A., Driessen, M. R. M., and Ellis, T. (2016). "GC Preps: Fast and easy extraction of stable yeast genomic DNA," *Scientific Reports* 6(1). DOI: 10.1038/srep26863

Cheng, B., Kuang, S., Shao, G., Tian, Q., Gao, T., Che, X., Ao, H., Zhang, K., and Liu, F. (2023). "Molecular cloning and functional analysis of HnSaratin from *Hirudo nipponia*," *Gene* 869, 147401-147401. DOI: 10.1016/j.gene.2023.147401

Del, M., Lópezdellamary, F. A., and Fornue, E. D. (2002). "Antifungal protection and sizing of paper with chitosan salts and cellulose ethers. Part 1, Physical effects," *Journal of the American Institute for Conservation* 41(3), 243-254. DOI: 10.1179/019713602806082584

Du, C., Wang, Y., Li, B., Xu, M., and Sadrizadeh, S. (2023). "Grey image recognition-based mold growth assessment on the surface of typical building materials responding to dynamic thermal conditions," *Building and Environment* 243, 110682-110682. DOI: 10.1016/j.buildenv.2023.110682

Farshid Mirzaee, Rezaei, S., and Samadyar, N. (2021). "Numerical solution of two-dimensional stochastic time-fractional Sine–Gordon equation on non-rectangular domains using finite difference and meshfree methods," *Engineering Analysis with Boundary Elements* 127, 53-63. DOI: 10.1016/j.enganabound.2021.03.009

Feng, Z.-X., Ren, Z.-C., and Li, J.-W. (2015). "An air-conditioning load forecasting based on dynamical combined residual error correction," *The Open Automation and Control Systems Journal* 7(1), 1441-1449. DOI: 10.2174/1874444301507011441

Gao, W., and Yang, H. (2022). "Time-varying Group Lasso Granger causality graph for high dimensional dynamic system," *Pattern Recognition* 130, 108789-108789. DOI: 10.1016/j.patcog.2022.108789

Gobakken, L. R., and Westin, M. (2008). "Surface mould growth on five modified wood substrates coated with three different coating systems when exposed outdoors," *Int. Biodeter. Biodegrad.* 62(4), 397-402. DOI: 10.1016/j.ibiod.2008.03.004

Gradeci, K., Labonnote, N., Time, B., and Köhler, J. (2017). "Mould growth criteria and design avoidance approaches in wood-based materials – A systematic review," *Construction and Building Materials* 150, 77-88. DOI: 10.1016/j.conbuildmat.2017.05.204

Higashijima, K., Wada, T., Igarashi, K., Enomae, T., Samejima, M., Isogai, A., and Igarashi, K. (2012). "Identification of filamentous fungi in paper damaged by tsunami of the Great East Japan Earthquake," *Japan TAPPI Journal* 66(9), 1008-1016. DOI: 10.2524/jtappij.66.1008

Hwang, J., Hari, A., Cheng, R., Gardner, J. G., and Lobo, D. (2020). "Kinetic modeling of microbial growth, enzyme activity, and gene deletions: An integrated model of β-glucosidase function in *Cellvibrio japonicus*," *Biotechnology and Bioengineering* Wiley, 117(12), 3876-3890. DOI: 10.1002/bit.27544

Jia, T., Liu, K., Li, Y., Cheng, Q., Cao, W., Luo, H., Ma, J., and Zhang, L. (2024). "Differential metabolites regulate the formation of chromatic aberration in *Toona fargesii* wood," *Industrial Crops and Products* 219, article 119021. DOI: 10.1016/j.indcrop.2024.119021

Kaminski, S., Evagelos Kirgios, André Bardow, and Leonhard, K. (2017). "Improved property predictions by combination of predictive models," *Industrial and Engineering Chemistry Research* 56(11), 3098-3106. DOI: 10.1021/acs.iecr.6b03125

Korzilius, S., and Schoenmakers, B. (2023). "Divisions and square roots with tight error analysis from Newton–Raphson iteration in secure fixed-point arithmetic," *Cryptography* 7(3), 43. DOI: 10.3390/cryptography7030043

Kosel, J., Legan, L., Bračič, M., and Ropret, P. (2024). "Cationic silicone based paper impregnation agent for the protection of historical paper against fungal growth. Detection and quantification of fungi using micro-invasive fluorescence microscopy and non-invasive FTIR spectroscopy," *Journal of Cultural Heritage* 68, 195-204. DOI: 10.1016/j.culher.2024.06.001

Kwon, S., Zambrano, M. C., Pawlak, J. J., and Venditti, R. A. (2021). "Effect of ligno-cellulosic fiber composition on the aquatic biodegradation of wood pulps and the isolated cellulose, hemicellulose and lignin components: Kinetic modelling of the biodegradation process," *Cellulose* 28(5), 2863-2877. DOI: 10.1007/s10570-021-03680-6

Liu, M., Liu, Y., Wang, Q., He, Q., and Geng, D. (2024). "Real-time detection technology of corn kernel breakage and mildew based on improved YOLOv5s," *Agriculture* 14(5), 725-725. DOI: 10.3390/agriculture14050725

Long, F.-Y., Qin, L.-W., Xiao, Y.-P., Hyde, K. D., Wang, S.-X., and Wen, T.-C. (2021). "Multigene phylogeny and morphology reveal a new species, *Ophiocordyceps vespulae*, from Jilin Province, China," *Phytotaxa* Q15088586, 478(1), 33-48. DOI: 10.11646/phytotaxa.478.1.2

Lõoke, M., Kristjuhan, K., and Kristjuhan, A. (2017). "Extraction of genomic DNA from yeasts for PCR-based applications," *BioTechniques* 62(1). DOI: 10.2144/000114497

Matysik, S., Herbarth, O., and Mueller, A. (2008). "Determination of volatile metabolites originating from mould growth on wall paper and synthetic media," *Journal of Microbiological Methods* 75(2), 182-187. DOI: 10.1016/j.mimet.2008.05.027

Menicucci, F., Palagano, E., Michelozzi, M., and Ienco, A. (2023). "Essential oils for the conservation of paper items," *Molecules* 28(13), 5003-5003. DOI: 10.3390/molecules28135003

Morsy, N., and Holiel, A. A. (2023). "Color difference for shade determination with visual and instrumental methods: A systematic review and meta-analysis," *Systematic Reviews* 12(1). DOI: 10.1186/s13643-023-02263-9

Ozcan, A., Sonmez, S., and Tutak, D. (2022). "Effect of coating pigment type on paper printability with water-based inks," *Journal of Coatings Technology and Research* 19(4), 1149-1157. DOI: 10.1007/s11998-021-00593-8

Quan, X. X., Yang, J. F., and Luo, Z. (2021). "Models in digital business and economic forecasting based on big data IoT data visualization technology," *Personal and Ubiquitous Computing*. DOI: 10.1007/s00779-021-01603-7

Revi, M., Badeka, A., Kontakos, S., and Kontominas, M. G. (2014). "Effect of packaging material on enological parameters and volatile compounds of dry white wine," *Food Chemistry* 152, 331-339. DOI: 10.1016/j.foodchem.2013.11.136

Saada, N. H., Othman, N. M., and None Mona Khaleil. (2022). "Author response for 'Mold-deteriorated archaeological Egyptian papyri: Biodeteriogens, monitoring the deterioration and treatment approach,'" *Archaeometry* 65. DOI: 10.1111/arcm.12831/v2/response1

Saif, F. A., Yaseen, S. A., Alameen, A. S., Mane, S. B., and Undre, P. B. (2020). "Identification of *Penicillium* species of fruits using morphology and spectroscopic methods," *Journal of Physics: Conference Series* 1644(1), article 012019. DOI: 10.1088/1742-6596/1644/1/012019

Sandberg, C. (2021). "Fibre development in an intensified mechanical pulping process," *Holzforschung* 75(9), 824-837. DOI: 10.1515/hf-2020-0242

Seto, K., D. Rabern Simmons, C. Alisha Quandt, Thijs Frenken, Dirks, A. C., Clemons, R. A., McKindles, K. M., McKay, M. L., and James, T. Y. (2023). "A combined microscopy and single-cell sequencing approach reveals the ecology, morphology, and phylogeny of uncultured lineages of zoosporic fungi," *MBio*. DOI: 10.1128/mbio.01313-23

Sun, H., Chen, J., Xiong, D., and Long, M. (2023). "Detoxification of Selenium yeast on mycotoxins and heavy metals: A review," *Biological Trace Element Research*. DOI: 10.1007/s12011-023-03576-5

Su, Y., and Zhao, H. (2023). "Infiltration approach of green environmental protection education in the view of sustainable development," *Sustainability* 15(6), article 5287. DOI: 10.3390/su15065287

Wang, C., Mei, Y., Wang, H., Guo, X., Yang, T., Du, C., and Yu, W. (2024). "A predictive model for the growth diameter of mold under different temperatures and relative humidities in indoor environments," *Buildings* 14(1), article 215. DOI: 10.3390/buildings14010215

Yu, G., Sun, Z., Peng, J., Zhu, M., Che, Q., Zhang, G., Zhu, T., Gu, Q., and Li, D. (2019). "Secondary metabolites produced by combined culture of *Penicillium crustosum* and a *Xylaria* sp.," *Journal of Natural Products* 82(7), 2013-2017. DOI: 10.1021/acs.jnatprod.9b00345

Zaffora, B., Coisne, L., and Gérard, C. (2024). "Survival models to estimate time to visible mold growth on new paper-based food-contact materials under varying environmental conditions," *LWT* 193, article 115767. DOI: 10.1016/j.lwt.2024.115767

Zasada, A. A. (2020). "Detection and identification of *Bacillus anthracis*: From conventional to molecular microbiology methods," *Microorganisms* 8(1), article 125. DOI: 10.3390/microorganisms8010125

Article submitted: January 2, 2025; Peer review completed: February 1, 2025; Revised version received and accepted: February 6, 2025; Published: March 12, 2025.
DOI: 10.15376/biores.20.2.3315-3328